

FINAL REPORT

Generating Graphene Nanosheet Electrodes for Electroanalysis and Fuel Cells

Changming Li
Nanyang Technological University
Singapore 637457

08 October 2008

Report Documentation Page

Form Approved
OMB No. 0704-0188

Public reporting burden for the collection of information is estimated to average 1 hour per response, including the time for reviewing instructions, searching existing data sources, gathering and maintaining the data needed, and completing and reviewing the collection of information. Send comments regarding this burden estimate or any other aspect of this collection of information, including suggestions for reducing this burden, to Washington Headquarters Services, Directorate for Information Operations and Reports, 1215 Jefferson Davis Highway, Suite 1204, Arlington VA 22202-4302. Respondents should be aware that notwithstanding any other provision of law, no person shall be subject to a penalty for failing to comply with a collection of information if it does not display a currently valid OMB control number.

1. REPORT DATE 12 OCT 2008		2. REPORT TYPE FInal		3. DATES COVERED 04-05-2007 to 08-10-2008	
4. TITLE AND SUBTITLE Generating Graphene Nanosheet Electrodes for Electroanalysis and Fuel Cells				5a. CONTRACT NUMBER FA48690714042	
				5b. GRANT NUMBER	
				5c. PROGRAM ELEMENT NUMBER	
6. AUTHOR(S) Changming Li				5d. PROJECT NUMBER	
				5e. TASK NUMBER	
				5f. WORK UNIT NUMBER	
7. PERFORMING ORGANIZATION NAME(S) AND ADDRESS(ES) Nanyang Technological University,N1.3-B2-12, 70 Nanyang Dr.,Singapore 637457,Singapore,SN,637457				8. PERFORMING ORGANIZATION REPORT NUMBER N/A	
9. SPONSORING/MONITORING AGENCY NAME(S) AND ADDRESS(ES) AOARD, UNIT 45002, APO, AP, 96337-5002				10. SPONSOR/MONITOR'S ACRONYM(S) AOARD-074042	
				11. SPONSOR/MONITOR'S REPORT NUMBER(S)	
12. DISTRIBUTION/AVAILABILITY STATEMENT Approved for public release; distribution unlimited					
13. SUPPLEMENTARY NOTES					
14. ABSTRACT This report covers development of carbon layers for electronic devices. It consists of two main chapters. The first is titled ?Novel Mesoporous Carbon and Its Direct Electrochemistry Based Biosensor.? The second is titled ?Mesoporous Organic Polymer-Carbon Nanocomposites for High Enzymatic Glucos/O2 Fuel Cells.?					
15. SUBJECT TERMS graphene nanosheet, fuel cells electrode					
16. SECURITY CLASSIFICATION OF:			17. LIMITATION OF ABSTRACT Same as Report (SAR)	18. NUMBER OF PAGES 15	19a. NAME OF RESPONSIBLE PERSON
a. REPORT unclassified	b. ABSTRACT unclassified	c. THIS PAGE unclassified			

Chapter 1

Introduction

This report consists of two manuscripts that will be published in archival journals. They appear as Chapters 2 and 3. The first is titled “Novel Mesoporous Carbon and Its Direct Electrochemistry Based Biosensor.” The second is titled “Mesoporous Organic Polymer-Carbon Nanocomposites for High Enzymatic Glucos/O₂ Fuel Cells.”

Novel Mesoporous Carbon and Its Direct Electrochemistry Based Biosensor

Shu-Juan Bao ^{a,b}, Chang Ming Li ^{a*}, Chun-Xian Guo ^a, Jun Guo ^c

Abstract: A microwave irradiation approach by using well-ordered mesoporous silica powders (SBA-15) as the template and polyethylene glycol as the carbon precursor was investigated to fabricate a new mesoporous carbon material. The effects of carbonization conditions on the microstructure and surface morphology of the synthesized products were examined systematically by X-ray diffraction (XRD), Raman, field emission scanning electron microscopy (FESEM) and high resolution transmission electron microscopy

(HRTEM). The experimental results show that microwave approach not only can reduce the reaction time significantly, but also produce a unique mesoporous carbon with slack porous surface, large specific surface area (1040 m²/g), uniform pore structure and good hydrophilicity. Using hemoglobin (Hb) as a model, the as-synthesized new carbon was explored for a direct electrochemistry based biosensor by immobilization of Hb. In comparison to the reported pure carbon materials and our previous work, Hb immobilized in the carbon shows more facile direct

electron transfer and better electrocatalytic performance without any electron transfer mediator in H₂O₂ biosensor. This work demonstrates a simple and efficient method to fabricate a novel high performance mesoporous carbon with fast direct electrochemistry of proteins and could provide potential applications in sensitive protein based biosensors, particularly electrochemical enzymatic sensors.

Keywords: Carbons; Biosensors; Enzymes; Electrocatalysis

Introduction

The achievement of mediator-free electron transfer between the prosthetic group of a redox protein and an electrode surface is of great interest in both fundamental investigations of biological redox reactions and practical applications of novel biosensors.^[1-3] The direct electrochemistry of proteins may provide a model to study the mechanism of electron transfer in various biological systems, and to create an efficient energy converting path for sensitive biosensors or superior bioreactors. Unfortunately, the direct electron transfer between redox protein and bare or "naked" solid electrode is very difficult. This is mainly caused by the redox centers deeply buried in the proteins, and also by the unfavourable orientations or denature of the proteins on electrode surfaces.^[4-5] It is highly desirable to fabricate unique nanostructured electrode materials or/and modify electrode surfaces for efficient protein immobilization with retaining favourable orientation, high bioactivity and fast electron transfer ability, leading to the direct electrochemistry.^[6-8]

Construction of materials with tailored textures has brought a great momentum to bioelectroanalysis.^[9-13] Particularly, the non-siliceous porous-structured materials have been used to modify electrodes and further to impregnate biomolecules for sensitive biosensors because of their high specific surface area and uniform pore distribution.^[10-13] The mesoporous structure may shorten the diffuse distance for the substrate to access the redox centers of the immobilized proteins and then to promote the direct electron transfer between the redox protein and the electrode surface.^[14-15] Among those porous materials, mesoporous carbon is a very important versatile material due to its low cost, high surface area, large pore volume, chemical inertness and conductive properties.^[16-18] A good electrode material should possess not only the high porosity and large surface area, but also the strong hydrophilicity, slack surface and good conductivity. These still remain great scientific challenges in research and development.

During the last decade, significant efforts have been devoted to synthesis of the mesoporous carbons utilizing the "nanocasting" technique, which involves impregnation of a porous silica template with an appropriate carbon source, carbonization of the carbon precursor, and subsequent removal of the template. A highly ordered mesoporous carbon, CMK-1 was synthesized by carbonization of the impregnated sucrose inside the pore channels of a mesoporous silica template at high temperature (>800 °C) followed by removal of the silica framework.^[19] Up to date, different structured porous silica templates and carbon precursors including furfuryl alcohol,^[20] phenol,^[21] and aromatic hydrocarbons^[22] have been developed to fabricate the high order carbons. However, the high carbonization temperature usually leads to products containing limited oxygen-based functional groups and then results in hydrophobicity from loss of oxygen-based functionality (e.g., alcohols). The increased

[a] Prof Chang Ming Li, Dr Shu-Juan Bao, Mr Chun-Xian Guo
School of Chemical and Biomedical Engineering and Center for Advanced
Bionanosystems, Nanyang Technological University, Nanyang Avenue, Singapore
639798
Fax: (+65 6791 1761
E-mail: ecml@ntu.edu.sg

[b] Dr Shu-Juan Bao
Institute of Applied Chemistry, Xinjiang University, Urumqi, 830046, P. R. China

[c] Ms Jun Guo
School of Materials Science and Engineering, Nanyang Technological University,
Nanyang Avenue, Singapore 639798

hydrophobicity prohibits the analyte to access the active sites of the proteins on the electrode surface.^[10] Clearly, this drawback can be a major barricade of the direct electron transfer at a protein/electrode interface. Recently, in order to enhance the hydrophilicity of the carbon materials, a number of methods have been explored by modifying the carbon surface, such as oxidation of carbons with nitric acids or ozone for producing some oxygenated functionalities. However, these methods could decrease the surface reactivity and damage the pore structure of the carbons during the oxidation treatment.^[23-25]

In this work, a novel method with using SBA-15 as the template and polyethylene glycol as the carbon precursor under microwave irradiation was developed to synthesize the mesoporous carbon. Compared with conventional heating methods, the microwave heating can deliver the energy to the materials through molecular interactions with electromagnetic field, resulting in uniform, rapid and volumetric heating without sacrificing the quality of the product.^[26] The mesoporous carbon fabricated by this method was systematically characterized by XRD, Raman, SEM, TEM, FTIR, nitrogen adsorption-desorption isotherms/pore-size distribution and contact angle measurements. The direct electrochemistry of redox proteins on the new material-modified electrode was investigated and a biosensor application was also explored to demonstrate the power of the synthesized new material.

Results and Discussion

The structural ordering of the as-synthesized carbon materials obtained under different carbonization conditions was first evaluated by XRD. The XRD pattern of the material prepared under microwave treatment for 15 min (Figure 1a) displays a weak peak of (100) and a broad peak at 2θ ranging from 1.7 to 1.98°, which is due to the overlap of two additional peaks of (110) and (200), indicating a ordered 2-d hexagonal structure.^[27] As shown in Figure 1b, with microwave treatment for 30 min, the intensity of the three well-defined peaks in the low-angle region increases significantly, which is very similar to that of the carbon material synthesized by conventional synthesis (Figure 1c). This suggests that a well ordered mesoporous structure of the sample similar to the carbon material fabricated by conventional synthesis was obtained. The high-angle XRD patterns of the samples exhibit two peaks, possibly associated with the graphite-like structure, i.e., (002) and (101) planes. The (002) peak of the carbons synthesized by different carbonization conditions should correspond to the carbon interlayer distance.^[28] The d_{002} value for the carbon obtained by microwave treatment 30 min is very close to that of the carbon prepared by conventional synthesis. This result indicates that the microwave method used in this work can reduce the reaction time significantly without sacrificing the quality of the products.

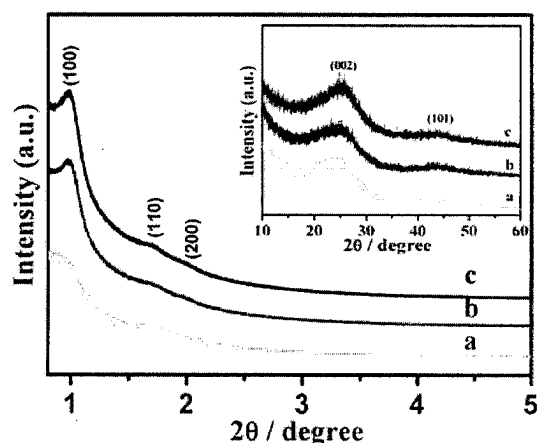


Figure 1 XRD patterns for as-synthesized carbon materials. The inset shows the high-angle XRD patterns of the samples. (a, Carbon obtained by microwave treatment for 15 min; b, Carbon obtained by microwave treatment for 30 min; c, Carbon obtained by conventional synthesis.)

Representative Raman spectra (Figure 2) of the carbons prepared with different carbonization conditions exhibit two bands at $\sim 1357\text{ cm}^{-1}$ (D band) and $\sim 1587\text{ cm}^{-1}$ (G band). The peak at 1587 cm^{-1} corresponds to an E_{2g} mode of the hexagonal graphite and is related to the vibration of sp^2 -bonded carbon atoms in a 2-dimensional lattice, such as in a graphite layer. The D-band at about 1357 cm^{-1} is associated with vibrations of carbon atoms with dangling bonds in plane terminations of disordered graphite or glassy carbons.^[27, 29] According to the Raman spectra results, the carbons are not fully graphitized under the three different carbonization conditions. Some disordered carbon or defects in the samples are illustrated by the result. The I_D/I_G ratios of the carbons prepared by conventional synthesis, microwave treatment for 30 min and 15 min are 0.81, 0.65, and 0.98, respectively. This result shows that more disordered carbon is present in the bulk sample synthesized with microwave treatment for 15 min, which is in accordance with the XRD results. The sample prepared by the microwave treatment for 30 min is more ordered than other two samples, further demonstrating that the microwave treatment is a good carbonization method for the synthesis of a mesoporous carbon.

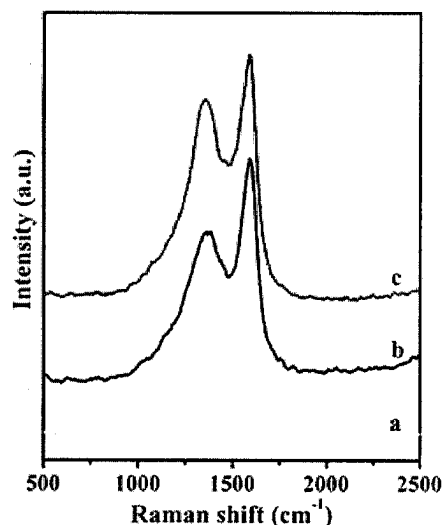


Figure 2 Raman spectra of as-synthesized carbon materials (a, Carbon obtained by microwave treatment for 15 min; b, Carbon obtained by microwave treatment for 30 min; c, Carbon obtained by conventional synthesis).

The effect of carbonization condition on the microstructure and morphology of the synthesized material was studied by FESEM. SBA-15 silica, the template used in the experiments, illustrates rope-like morphologies with a relatively uniform size (Figure 3a). Its high-resolution SEM image reveals that the external surface of the SBA-15 silica is composed by a uniform array of parallel channels (Figure 3b). The SEM images of the carbon prepared by conventional synthesis with SBA-15 silica template exhibit very similar morphologies to those of the template (Figure 3c and 3d). However, the sample obtained by the microwave treatment for 15 min displays a very different morphology that consisted of amorphous flakes, most likely due to a lower growth rate (Figure 3e and 3f). Interestingly, when the microwave treatment time increases to 30 min, the sample tends to form loose and porous bundles (Figure 3g) composed of very thin paralleled nanowires (Figure 3h). The detail structure of the mesoporous carbon fabricated under different carbonization conditions was investigated by TEM and high magnification FESEM.

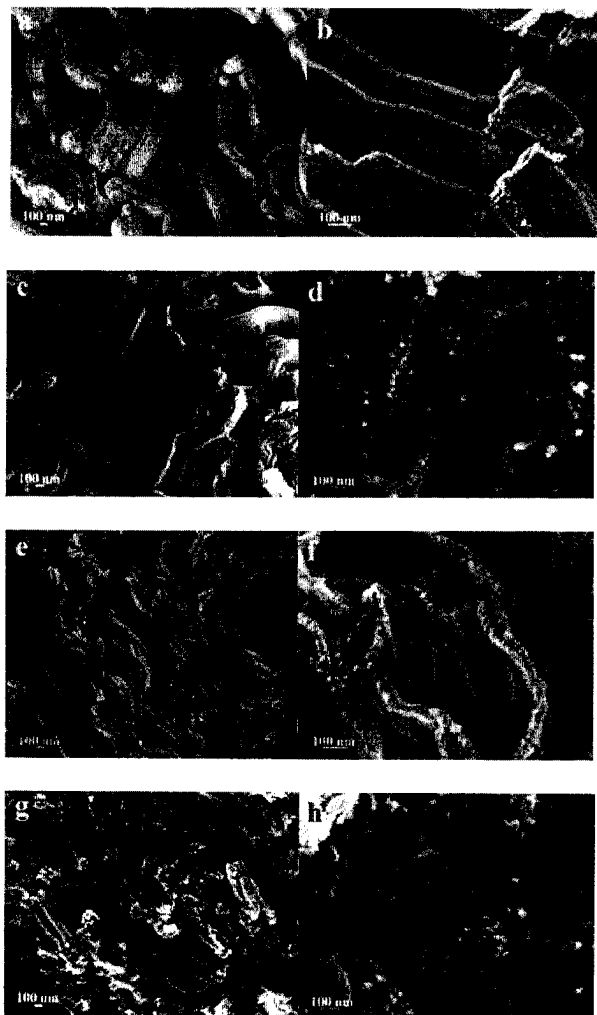


Figure 3 Low and high magnification FESEM of the samples. (a and b, SBA-15; c and d, Carbon prepared by conventional synthesis; e and f, Carbon obtained by microwave treatment for 15 min; g and h, Carbon obtained by microwave treatment for 30 min.)

The representative TEM images of the carbon materials synthesized under different heating methods are shown in Figure 4. As displayed in Figure 4b and 4e, both of the samples have well-ordered mesoporous structures. The relatively bright lines are the images of nanopores of the carbon, while the black lines are carbon wires filled in the pores of SBA-15 (Figure 4b, 4e and 4f). However, the samples fabricated by different heating methods also present significantly different microstructures (Figure 4a and 4c); the surface of the carbon produced by the microwave treatment for 30 min. is more slack and porous than the material prepared by the conventional synthesis. The high-magnification TEM further illustrates that the slack surface of the carbon formed by the microwave treatment for 30 min. is composed of uniformly distributed mesostructured cells with a diameter of ~10 nm (Figure 4d). The pore diameter can be readily tuned to match the dimensional size of diverse biomolecules (< 8 nm), making the material suitable for protein immobilization.^[10]

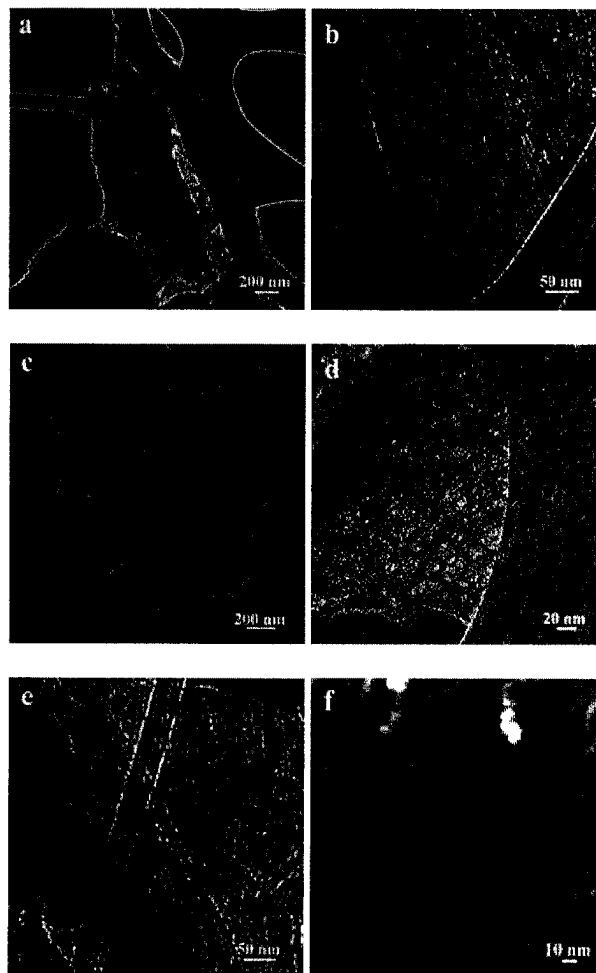


Figure 4 TEM (a and b) images of carbon obtained by conventional synthesis; TEM (c, d and e) and FESEM (f) images of carbon obtained by microwave treatment for 30 min.

In Figure 5, the nitrogen adsorption-desorption isotherms and pore-size distribution measured from different mesoporous carbons are compared with those of SBA-15 silica. The ordered SBA-15 silica shows type IV with type H₁ hysteresis loops for a typical mesoporous and well-organized hexagonal structure with amorphous pore walls and narrow pore size distributions centered at 6.3 nm. The specific surface area for silica SBA-15 is 821 m²/g, and little micropores are present in its pore structure. The structure of the silica template can determine the primary structure of the resulted mesoporous carbon because the space occupied by the silica framework forms the mesopores after the removal of the silica template. The nitrogen adsorption-desorption isotherm for the mesoporous carbon prepared by the conventional synthesis in Figure 5a(II) displays a reverse replica of the SBA-15 ordered silica with hexagonal structure, which is analogous to the ordered mesoporous carbon reported.^[27] Comparison of two carbon materials prepared under different microwave treatment times shows that the adsorption capacity increases and the position of the capillary condensation step shifts to relatively higher pressures as the microwave treatment time increases. The BET surface area of the carbon prepared by the microwave treatment for 30 min is 1040 m²/g, larger than that of the carbon synthesized under a shorter time of 15 min (775 m²/g), and also the carbon synthesized by the conventional method (884 m²/g). The results clearly demonstrate that this simple microwave approach can maintain the microstructure, high surface area and uniform pore size distribution of the template in the prepared carbons and even much small pores (< 3 nm) in the carbon prepared by the microwave treatment for 30 min (Figure 5b(III)). It is recently reported that the small pores could be a stoichiometric electron acceptor and host for a variety of electron-donating guest species, and thus is favorable to a wide variety of reactions involving electron transfer to a non-siliceous mesoporous host lattice. Hence, the unique structure could be used to immobilize proteins for direct electrochemistry.^[30-32]

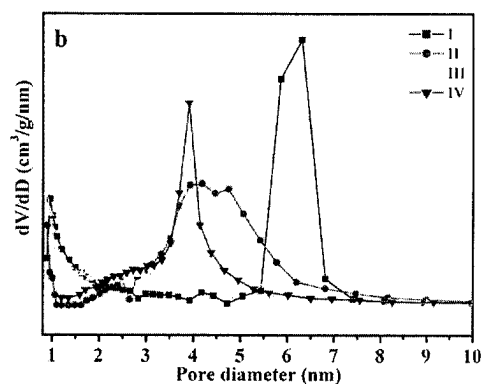
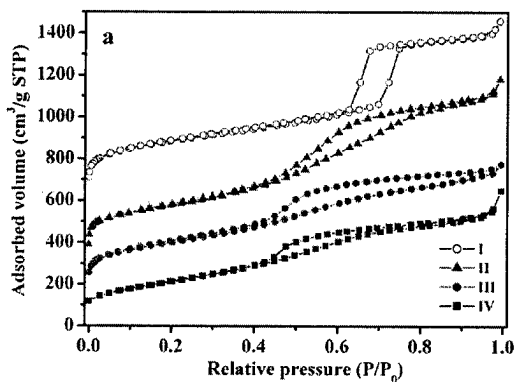


Figure 5(a) Nitrogen adsorption-desorption isotherms of SBA-15 silica (I) and carbon obtained by different carbonization conditions; (b) BJH pore-size distributions of SBA-15 silica (I) and carbon obtained by different carbonization conditions (II, Carbon prepared by conventional synthesis; III, Carbon obtained by microwave treatment for 15 min; IV, Carbon obtained by microwave treatment for 30 min).

The hydrophilicity of the carbons fabricated in this work was evaluated by water contact angle measurements. The water contact angles of the carbons obtained by the microwave treatments for 15, 30 min and conventional approach were 9.3 °, 23 ° and 38.6 °, respectively, which were much smaller than 79.1 ° observed for the mesoporous carbon material reported in literature.^[10] This could be explained by FTIR spectra of the samples shown in Figure 6. The broad absorption bands centered at 3450 and 1620 cm⁻¹ correspond to the stretching and bending modes of the OH group, and the absorption bands at 1234 and 1385 cm⁻¹ are assigned to the stretching and bending vibrations of C-OH. The results indicate that the hydroxyl group still remains in the prepared carbons with polyethylene glycol as carbon precursor. Apparently, the remaining hydroxyl group could improve the hydrophilicity of the mesoporous carbon for soluble analytes to access the active sites of enzymes and then to achieve better biocatalysis.

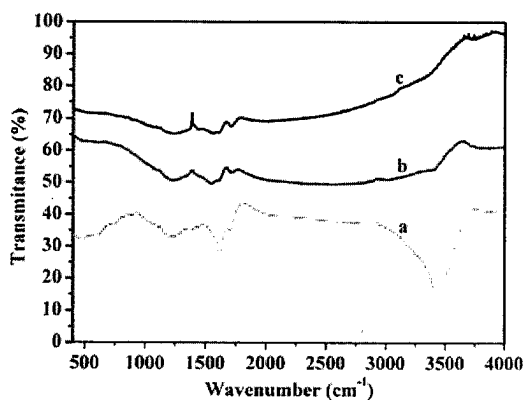


Figure 6 FTIR spectra of the carbons obtained by different carbonization conditions (a, Carbon obtained by microwave treatment for 15 min; b, Carbon obtained by microwave treatment for 30 min; c, Carbon prepared by conventional synthesis).

Due to its unique porous structure, large surface area and good hydrophilicity, the mesoporous carbon prepared by microwave

5

treatment for 30 min was further explored for protein direct electrochemistry based biosensing, in which Hb, a protein that stores and transports molecular oxygen in mammalian blood, was selected as a model molecule to detect the electrocatalytic current for H_2O_2 reduction.

Cyclic voltammogram (CV) was employed to study the possibility of direct electrochemistry of Hb on the mesoporous carbon. The voltammograms measured on various electrode surfaces in nitrogen saturated PBS buffer solution in Figure 7 show a pair of well-defined redox peaks for the Hb-mesoporous carbon modified glass carbon (GC) electrode (curve c), but no obvious redox peaks for both Hb and mesoporous carbon alone modified electrodes (curves a and b). The redox potential shown in curve c is very close to the characteristic one of $\text{Fe}^{\text{III}}/\text{Fe}^{\text{II}}$ redox couple of the heme protein^[33] The Hb immobilized mesoporous carbon clearly demonstrates the direct electron transfer ability. The anodic peak potential (E_{pa}) and the cathodic peak potential (E_{pc}) are located at -0.323 V and -0.371 V, respectively, corresponding to a peak-to-peak separation (ΔE_{p}) of 48 mV and a formal potential (E^0) of -0.347 V calculated with $E^0 = 1/2(E_{\text{pa}} + E_{\text{pc}})$. The small value of ΔE_{p} indicates a fast electron-transfer rate for Hb-mesoporous carbon GCE.

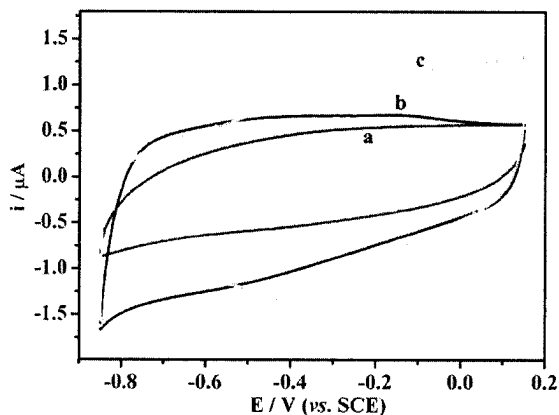


Figure 7 Cyclic voltammograms of different materials modified GCEs in 0.01 M pH 7.4 nitrogen-saturated phosphate buffered saline (PBS) solution at 100 mV/s. (a, Hb/Nafion; b, mesoporous carbon/Nafion; c, mesoporous carbon/Hb/Nafion). (GCE: glass carbon electrode; SCE: saturated calomel electrode).

The effect of the scan rate on the electrochemical response of the Hb-mesoporous carbon modified electrode is shown in Figure 8. Within the scan rate range of 100 to 800 mV/s, the reduction and oxidation peak currents exhibit a linear relationship against the scan rate (shown in Figure 8b with $r=0.996$). The charge consumed in coulombs, Q (obtained from integrating the anodic or cathodic peak area in CVs), with the background correction, is invariable at different scan rates. These results confirm that the electrochemical reaction of Hb on the mesoporous carbon exhibits a surface-controlled behavior, in which all electroactive ferric proteins (protein- Fe^{III}) produced by the oxidation of ferrous proteins (protein- Fe^{II}) on the anodic scan could be reduced to protein- Fe^{II} on the cathodic scan. The surface concentration of the electroactive Hb (Γ^*) in the mesoporous carbon could be calculated by integrating CV reduction peak based on the formula of $Q = nF\Gamma^*A$, where A is the effective area of GC electrode (0.07 cm^2) and other symbols have their known usual meanings. The average Γ^* value over the

scan rate range is $7 \times 10^{-10} \text{ mol cm}^{-2}$. In addition, the apparent heterogeneous electron transfer rate constant k_s of Hb in the mesoporous carbon modified electrode could be estimated by using the equation derived by Laviron for diffusionless CV.^[34] The calculated value of k_s , 5.3 s^{-1} indicates the Hb at the mesoporous carbon modified electrode has faster electron transfer rate than that observed from Hb immobilized on black carbon (1.02 s^{-1}), CNTs (0.062 s^{-1}), PANI/mesoporous carbon (2.07 s^{-1}), also our previous work.^[35-39]

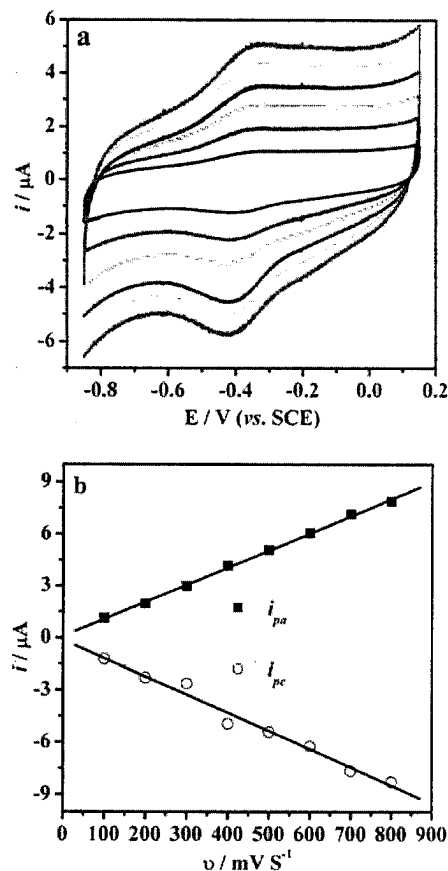


Figure 8 a, Cyclic voltammograms of Hb-mesoporous carbon modified GC electrode in a 0.01 M PBS buffer (pH 7.4) at different scan rates (from 100 to 600 mV/s, inside to outside). b, The plots of the reduction and oxidation peak currents i against the scan rate v .

Based on its direct electrochemistry behavior, the Hb-mesoporous carbon modified electrode was employed to electrocatalyze H_2O_2 reduction for a sensitive biosensor. The catalytic reduction peak of H_2O_2 at Hb-mesoporous carbon modified electrode is shown in Figure 9, in which the half-wave potential of H_2O_2 reduction is very close to the redox potential of the reversible electrochemical reaction for the direct electron transfer between Hb and electrode. After addition of H_2O_2 in the test solution, the reduction peak current of Hb increases, accompanied by the decrease and even disappearance of the oxidation peak, indicating the reduction of H_2O_2 is catalyzed by the Hb immobilized in the mesoporous carbon.

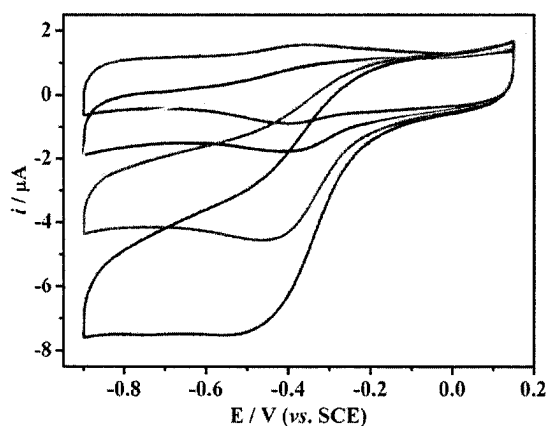


Figure 9 Cyclic voltammograms of Hb-mesoporous carbon modified GC electrode in a 0.01 M PBS buffer (pH 7.4) containing different H_2O_2 concentrations at 100 mV/s. (0 μM , 6.7 μM , 13 μM , 27 μM , 53 μM ; from up to down.)

The relationship between the reduction peak current and the H_2O_2 concentration is displayed in Figure 10. The respective peak current changes linearly with the H_2O_2 concentration (inset) ranging from 1.3×10^{-6} to 4×10^{-5} M ($R=0.996$), with a reactive sensitivity of $0.15 \mu\text{A} \mu\text{M}^{-1}$, which makes it possible to fabricate an Hb based H_2O_2 biosensor. The detection limit is 2.2×10^{-7} M. When the concentration of H_2O_2 is higher than 7.7×10^{-6} M, the calibration curve tends to a plateau and then drops down with further adding H_2O_2 , implying a progressive enzyme inactivation at the presence of higher concentration of H_2O_2 that coincided with a Michaelis-Menten kinetics model.^[34]

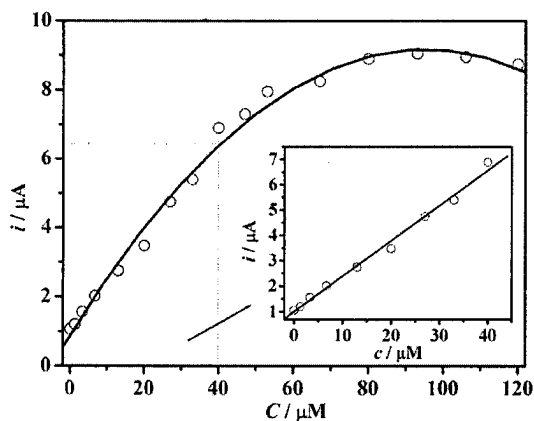


Figure 10 Calibration curve of the reduction peak current against the concentration of H_2O_2 . The inset is the linear relative plot.

Conclusion

This work demonstrated a novel and effective microwave irradiation method to fabricate a new mesoporous carbon with very slack porous surface, large specific surface area ($1040 \text{ m}^2/\text{g}$) and good hydrophilicity. The effects of the carbonization conditions on the microstructure and surface properties of the products were investigated. The results show that microwave approach not only can reduce the reaction time significantly, but also produce slack porous surface in the carbon bundles. The slack porous surface

coupled with good hydrophilicity and small pore channels of the material is very suitable to be effectively immobilized by proteins and promotes the direct electron transfer at a protein/electrode interface. Hb immobilized on the material exhibited much more facile direct electrochemistry and better electrocatalytic performance without any electron transfer mediator than the reported pure carbon materials. The enhanced direct electron transfer of Hb at the slack mesoporous carbon modified electrode is very likely contributed by the unique nanostructure, hydrophilic surface and pore structure of the new synthesized carbon material. The direct electrochemistry based H_2O_2 biosensor shows a good sensitivity. The novel textile form and porous nanostructure nature may also make the material feasible in application explorations for double layer capacitor, lithium ion battery, and catalyst support. Further researches to optimize the synthesis conditions for different applications of this material such as in lithium ion battery and fuel cells is currently undergoing in our lab.

The authors are grateful to the Asian Office of Aerospace Research and Development, Department of The Air Force of USA for the financial support to this work under contract of FA5209-05-P-0505.

Experimental Section

Material Synthesis: All the chemicals were of analytical grade and used without further purification. The new mesoporous carbon was synthesized by using SBA-15 silica (purchased from Jilin University High-Tech. Co. Ltd., Changchun, China) as template and polyethylene glycol (PEG) as carbon precursor under microwave irradiation. The process could be described as follows: 1 g SBA-15 silica was first dispersed into 10 mL PEG 400 under ultrasonic for 1 h, and then PEG was infiltrated into the channels of SBA-15 silica adequately in a vacuum of 0.1 MPa for 2 h. The obtained mixture was stored at atmosphere overnight for silica depositing. After removal of the redundant PEG, a viscous gel was obtained. 1 mL H_2SO_4 was dropped into the viscous gel under vigorous stirring. The obtained precursor was placed in a drying oven for 12 h at 150°C . The carbonization was completed at microwave oven (LG, MS-2744B) using graphite as heat-conducting layer for different time. The carbonization was carried out in a procedure of 5 min on and 1 min off and 5 min on again. After 15 min microwave treatment, a black sample was obtained; After 30 min microwave treatment, a grey sample was obtained. When the time increases to 45 min, the product changed to white completely, indicating the carbon precursor which infiltrated into the channels of SBA-15 silica also disappeared. So, in this work, the carbonization time was selected lower than 30 min. Finally the carbon/silica composite obtained after carbonization was washed with 5 wt% hydrofluoric acid at room temperature to remove the silica template. For comparison, the material was also pyrolyzed according conventional method, at 900°C under N_2 flow for 3 h.

Material Characterization: The crystal structure of the product was characterized by X-ray diffraction (XRD, Bruker AXS X-ray diffractometer). Morphology and microstructure of the synthesized materials were investigated by field emission scanning electron microscopy (FESEM, JSM-6700F, Japan) and high-resolution transmission electron microscope (HRTEM, JEM-2100F, Japan). Nitrogen adsorption/desorption experiments were carried out at 77.3 K by means of an Autosorb-1 (Quantachrome Instruments) analyzer. The surface area was calculated by using the Brunauer-Emmett-Teller (BET) equation. Pore-size distributions were calculated by the Barrett-Joyner-Halenda (BJH) method. Raman study of the samples was carried out by a setup with an integrated confocal Raman microscope system (CRM200, WITec, Germany).

Electrode Preparation and Measurement: Glassy carbon electrodes with 3mm in diameter (GCE, CH Instruments, USA) were polished with 0.3 and $0.05 \mu\text{m}$ alumina powder, followed by thorough rinsing with deionized water. After sonicating in 1 M nitric acid, acetone and deionized water, respectively, the electrodes were dried at room temperature.

10 mg new mesoporous carbon was dispersed into 2 mL double-distilled water under ultrasonic for 2 h. Then, 1 mL upper solution after depositing for 1 h was transferred into a fresh tube, followed by adding 10 mg Hb under ambient conditions and shaken 30 min. The mixture obtained above was finally stored at 4°C overnight for protein adsorption. Before each experiment, the bioconjugates obtained above were re-shaken, and then 2 μL of the suspension was deposited onto the centre of the pre-treated GCE. 3 μL of 0.5% Nafion was subsequently placed on the whole electrode surface to form

Nafion membrane, which was used to fix Hb impregnated materials on electrode. And then, the modified electrode was left to dry at room temperature.

The electrochemical measurements were carried out using a three-electrode system, employing a platinum wire as the counter electrode, a saturated calomel electrode (SCE) as the reference, and the new mesoporous carbon modified glassy carbon electrode (GCE) as the working electrode.

-
- [1] J. J. Wei, H. Y. Liu, A. R. Dick, H. Yamamoto, Y. F. He, D. H. Waldeck, *J. Am. Chem. Soc.* 2002, 124, 9591.
- [2] Y. Xiao, F. Patolsky, E. Katz, J. F. Hainfeld, I. Willner, *Science* 2003, 299, 1877.
- [3] M. K. Bessenhirtz, F. W. Scheller, W. F. M. Stocklein, D. G. Kurth, H. Mhwald, F. Lisdat, *Angew. Chem., Int. Ed.* 2004, 43, 4357.
- [4] C. Mu, Q. Zhao, D. Xu, Q. Zhuang, Y. Shao, *J. Phys. Chem. B* 2007, 111, 1491.
- [5] A. Riklin, E. Katz, I. Willner, A. Stocker, A.F. Buchmann, *Nature* 1995, 376, 672.
- [6] X. Q. Cui, C. M. Li, J. F. Zang, S. C. Yu, *Biosens. Bioelectron.* 2007, 22, 3288.
- [7] J. F. Zang, C. M. Li, X.Q. Cui, J. X. Wang, X. W. Sun, H. Dong, C. Q. Sun, *Electroanal.* 2007, 19, 1008.
- [8] C. M. Li, C. S. Cha, *Front. Biosci.* 2004, 9, 3324.
- [9] Y. Wang, F. Caruso, *Chem. Commun.* 2004, 1528.
- [10] S. Wu, H. Ju, Y. Liu, *Adv. Funct. Mater.* 2007, 17, 585.
- [11] S. J. Bao, C. M. Li, Z. J. Zang, X. Q. Cui, Y. Qiao, J. Guo, *Adv. Funct. Mater.* 2008, 18, 591.
- [12] Y. Qiao, S. J. Bao, C. M. Li, X. Q. Cui, Z. S. Lu, J. Guo, *ACS Nano.* 2008, 2, 113.
- [13] Y. Qiao, C. M. Li, S. J. Bao, *Chem. Commun.* 2008, 1290.
- [14] H. Zhu, E. W. Stein, Z. Lu, Y. M. Lvov, M. J. McShane, *Chem. Mater.* 2005, 17, 2323.
- [15] P. Yang, D. Zhao, D. I. Margolese, B. Chmelka, G. Stucky, *Nature* 1998, 396, 152.
- [16] X. Xu, B. Tian, J. Kong, S. Zhang, B. Liu, D. Zhao, *Adv. Mater.* 2003, 15, 1932.
- [17] S. Jun, S. H. Joo, R. Ryoo, M. Kruk, M. Jaroniec, Z. Liu, T. Ohsuna, O. Terasaki, *J. Am. Chem. Soc.* 2000, 122, 10712.
- [18] S. Che, K. Lund, T. Tatsumi, S. Iijima, S. H. Joo, R. Ryoo, O. Terasaki, *Angew. Chem. Int. Ed.* 2003, 42, 2182.
- [19] R. Ryoo, S. H. Joo, S. Jun, *J. Phys. Chem. B* 1999, 103, 7743.
- [20] S. H. Joo, S. J. Choi, I. Oh, J. Kwak, Z. Liu, O. Terasaki, R. Ryoo, *Nature* 2001, 412, 169.
- [21] R. Ryoo, I. S. Park, S. Jun, C. W. Lee, M. Kruk, M. Jaroniec, *J. Am. Chem. Soc.* 2001, 123, 1650.
- [22] J. Lee, K. Sohn, T. Hyeon, *J. Am. Chem. Soc.* 2001, 123, 5146.
- [23] Z. Li, W. Yan, S. Dai, *Langmuir*, 2005, 21, 11999.
- [24] T. A. Zwier, M. F. Burke, *Anal. Chem.* 1981, 53, 812.
- [25] J. L. Bahr, J. M. Tour, *J. Mater. Chem.* 2002, 12, 1952.
- [26] E. H. Hong, K. H. Lee, S. H. Oh, C. G. Park, *Adv. Funct. Mater.* 2003, 13, 961.
- [27] Z. Li, J. Zhang, Y. Li, Y. Guan, Z. Feng, C. Li, *J. Mater. Chem.* 2006, 16, 1350.
- [28] T. W. Kim, R. Ryoo, K. P. Gierszal, M. Jaroniec, L. A. Solovyov, Y. Sakamoto, O. Terasaki, *J. Mater. Chem.* 2005, 15, 1560.
- [29] Z. Sun, Z. Liu, J. Du, Y. Wang, B. Han, T. Mu, *J. Phys. Chem. B* 2004, 108, 9811.
- [30] M. Vettraino, M. L. Trudeau, D.M. Antonelli, *Adv. Mater.* 2000, 12, 337.
- [31] X. He, M. Trudeau, D.M. Antonelli, *Adv. Mater.* 2000, 12, 1036.
- [32] M. Vettraino, X. He, M. Trudeau, J. E. Drake, D. M. Antonelli, *Adv. Funct. Mater.* 2002, 12, 174.
- [33] G. Shi, Z. Sun, M. Liu, L. Zhang, Y. Liu, Y. Qu, L. Jin, *Anal. Chem.* 2007, 79, 3581.
- [34] E. Laviron, *J. Electroanal. Chem.* 1979, 101, 19.
- [35] G. X. Ma, T. H. Lu, Y. Y. Xia, *Bioelectrochem.* 2007, 71, 180.
- [36] Y. D. Zhao, Y. H. Bi, W. D. Zhang, Q. M. Luo, *Talanta*, 2005, 65, 489.
- [37] G. X. Ma, Y. G. Wang, C. X. Wang, T. H. Lu, Y. Y. Xia, *Electrochim. Acta*, 2008, 53, 4748.
- [38] Q. Lu, C. M. Li, *Biosens. Bioelectron.* 2008, doi:10.1016/j.bios.2008.06.056
- [39] C. X. Guo, F. P. Hu, C. M. Li, P. K. Shen, *Biosens. Bioelectron.* 2008, doi:10.1016/j.bios.2008.07.007

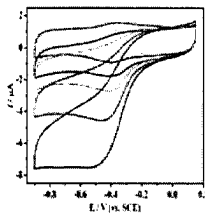
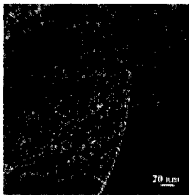
Received: ((will be filled in by the editorial staff))

Revised: ((will be filled in by the editorial staff))

Published online: ((will be filled in by the editorial staff))

Shu-Juan Bao^{a,b}, *ang Ming Li*
^a, *Chun-Xian Guo*^a, *Jun Guo*
^b

Novel Mesoporous Carbon and Its
Direct Electrochemistry Based
Biosensor



A novel mesoporous carbon with high specific surface area, unique nanostructure and good hydrophilicity is synthesized in our work. Hemoglobin (Hb) immobilized on the material exhibits facile, direct electrochemistry and good electrocatalytic performance without any electron mediator, indicating that the slack porous mesoporous carbon is an attractive material to fabricate biosensors, particularly enzymatic sensors.

Chapter 3

Mesoporous Organic Polymer-Carbon Nanocomposite for High Performance Enzymatic Glucose/O₂ fuel Cells

Chunxian Guo^{ab}, Fengping Hu^{ab}, Chang Ming Li^{ab*}

^a*School of Chemical and Biomedical Engineering, Nanyang Technological University, 70 Nanyang Drive, Singapore 637457, Singapore. E-mail: ECMLi@ntu.edu.sg; Fax: +65 6791 1761; Tel: +65 6790 4485*

^b*Centre for Advanced Bionanosystems, Nanyang Technological University, 70 Nanyang Drive, Singapore 637457, Singapore*

Enzymatic glucose/O₂ fuel Cell based on direct electron transfer of glucose oxidase on mesoporous organic polymer-carbon nanocomposite demonstrates excellent performance.

Miniaturized enzymatic glucose/O₂ fuel cells have roused great interest for the last two decades because of their potential role as power sources for drug delivery, microelectronics devices, and health monitoring and implant devices such as cardiac pacemakers.¹ Recently one of the most significant advances in glucose/O₂ fuel cells has been the development of bioanode or biocathode that employs direct electron transfer (DET) between enzymes and electrode surface due to its super simplicity for miniaturization and improved performance.² However, poor power density and short lifetime are still two main bottlenecks in their real applications, which demand solutions to overcome the following three hurdles.³ Firstly, electrodes must be high electronic and proton conductivity to support efficient charge transfer of immobilized enzymes and to minimize resistive losses.^{4,5} Secondly, electrodes should be three-dimensional with large specific surface area and suitable pore diameter to immobilize more enzymes and promote the mass transport of liquid phase fuel.⁶ Finally, electrodes should provide good microenvironment for long-term stability to prevent denaturing of immobilized enzymes.⁷ In this regard, porous nanostructured electrode materials with excellent conductivity, high surface area and suitable hydrophilicity are highly required.

Recently, great efforts have been expended in synthesis a new class of inorganic porous material, ordered mesoporous carbons (OMCs).⁸ Considering their unique properties, such as high surface area, large pore volume and narrow pore size distribution, OMCs have been widely used as host matrix for enzyme immobilization. However, high hydrophobicity and limited pore diameters of OMCs restrict their applications in fuel cells.^{6,9} Organic polymers with unique properties such as good biocompatibility and suitable hydrophilicity have been widely used in various applications.¹⁰ Unfortunately, the low mechanical strength and poor conductivity limit their applications as electrode materials for fuel cells. In this communication, an ordered mesoporous organic polymer-carbon nanocomposite with the bifunctionality of carbon and organic polymer was synthesized. The DET of glucose oxidase (GOD) on this composite was examined. Glucose/O₂ fuel cell based on this GOD anode and

Pt cathode was constructed and its performance was investigated. To the best of our knowledge, this novel nanocomposite is for the first time synthesized and applied to enzymatic glucose/O₂ fuel cells.

The present synthesis strategy is to impregnate organic polymer poly(vinyl alcohol) (PVA) into the carbon source and the molecular sieve (details in supporting information). The as-synthesized materials have been examined by microscopy, water contact angle and electrochemical measurement. Figure 1a and 1b show two transmission electron micrograph (TEM) images viewed along and perpendicular to the direction of the pore arrangement of the nanocomposite. The ordered pores are 6 nm in diameter, the centers of adjacent pores 10 nm apart and the surface-to-surface distance 4 nm, similar to the CMK-3 reported.¹¹ The surface area of the composite increases by 42% compared with mesoporous carbon obtained from nitrogen adsorption/desorption isotherm (supporting information). Figure 1c shows the water contact angle (CA) of composite and mesoporous carbon. It exhibits a contact angle of 26.8° for the composite almost equal to that of the PVA alone¹² while it shows an angle around 80° for mesoporous carbon. Figure 1d shows the electrochemical activities of as-synthesized materials characterized by electrochemical impedance spectroscopy (EIS). Randle equivalent circuit is used to model the complex impedance in the electrochemical cell.¹³ The values of charge-transfer resistance R_{ct} obtained are 5.2 and 17.5 $\Omega\text{ cm}^2$ for composite and mesoporous carbon electrode, respectively, indicating that composite electrode has much faster charge transfer rate.

With large surface area and matching pore size to enzyme glucose oxidase (GOD), the high conductive nanocomposite was used as host of GOD immobilization. The maximum loading of GOD was about 38 wt%, determined by UV-Vis spectra at 280 nm. The GOD loading capacity was about 4.5-fold higher than that the high hydrophobic mesoporous carbon (this work) and 10-fold higher than that CMK-3 with pore diameter of 4nm.¹⁴ The high GOD loading may come from its suitable hydrophilicity and pore size matching between GOD and the composite. Direct electron transfer of immobilized GOD on composite was tested by cyclic voltammeteries (CVs) in Figure 2a. The formal potential was -0.52 V versus Ag/AgCl, which is similar to the redox potential of the FAD/FADH₂ cofactor in the enzyme itself at pH 7.0. The electron transfer rate constant K_s , calculated from Laviron model is about 3.98 s⁻¹, which is larger than that observed on MWNTs (2.3 s⁻¹) and SWNTs (0.3 s⁻¹) electrodes.¹⁵ The reasons for the high K_s might lie in the fast charge transfer of the nanocomposite and the good interaction between GOD and the composite. The application of GOD/composite electrode as an anode was demonstrated by the polarization curves (Figure 2b) in a quiescent 30 mM glucose in pH 7.0 phosphate buffer solution in air at room temperature. Catalytic electrooxidation of glucose was observed at -0.6 V vs Ag/AgCl, and it reached its plateau of 150 $\mu\text{A cm}^{-2}$ near -0.5 V vs Ag/AgCl.

Glucose/O₂ fuel cell was constructed by applying the GOD/composite as anode and Pt electrode as cathode. The polarization curve of the cathode was shown in figure 2b. Catalytic electroreduction of O₂ was observed at +0.6 V vs Ag/AgCl and reached its 1200 $\mu\text{A cm}^{-2}$ near +0.4 V vs Ag/AgCl. The relationship between the power

//

density and the current density and the polarization curve of the assembled glucose/O₂ fuel cell was displayed in Figure 3. The open-circuit voltage was near 1.2 V and the power density was 0.11 mW/cm² at 0.72 V. When the cell operated continuously for in quiescent solution under ambient air, it lost ca. 10% of its power in the first 24 hours and then ca. 6% per day within the first week.

In conclusion, a mesoporous organic polymer-carbon nanocomposite with high surface, large pore diameter, suitable hydrophilicity and good conductivity was synthesized and the nanocomposite was successfully applied in glucose/O₂ fuel cell. With long term stability more than one week, the power density of the assembled glucose/O₂ fuel cell is the highest comparable to other glucose/O₂ fuel cells based on direct electron transfer reported thus far. This nanocomposite can also be used for the improvement of other kinds of fuel cells performance and a great prospect for practical applications.

The authors are grateful to the Asian Office of Aerospace Research and Development, Department of The Air Force of USA for the financial support to this work under contract of FA5209-05-P-0505.

Figures

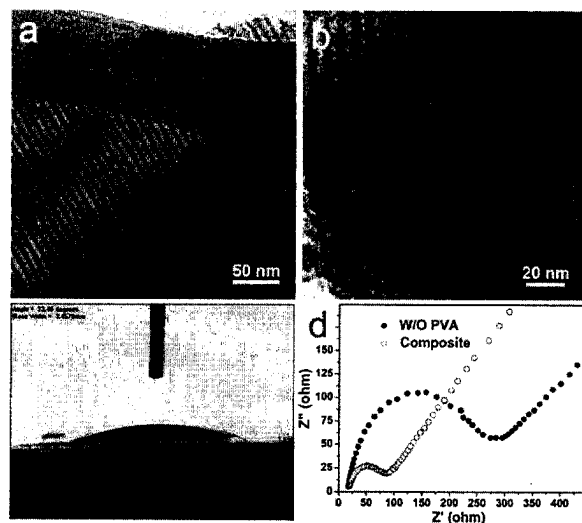


Figure 1. TEM image along (a) and perpendicular to the direction of the pore arrangement (b). (c) Photographs of water droplet on the composite. (d) Electrochemical impedance spectroscopy (EIS) of 10 mM Fe(CN)₆^{3-/4-} in 1.0 M KCl.

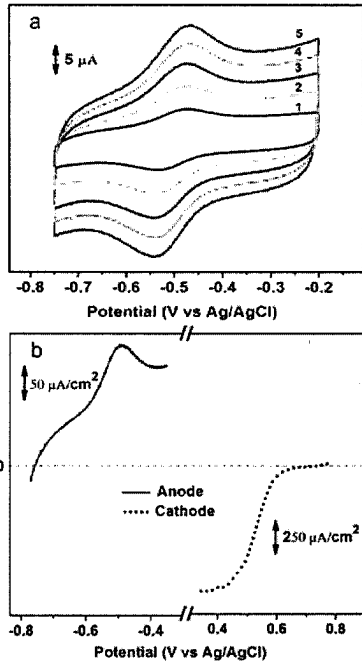


Figure 2. (a) Cyclic voltammograms (CV) of the GOD/composite electrode in 100 mM phosphate buffer, pH 7.0, at various scan rate, mV/s: (1) 50; (2) 100; (3) 150; (4) 200; (5) 250. (b) Polarization of the GOD/composite anode and of the Pt cathode.

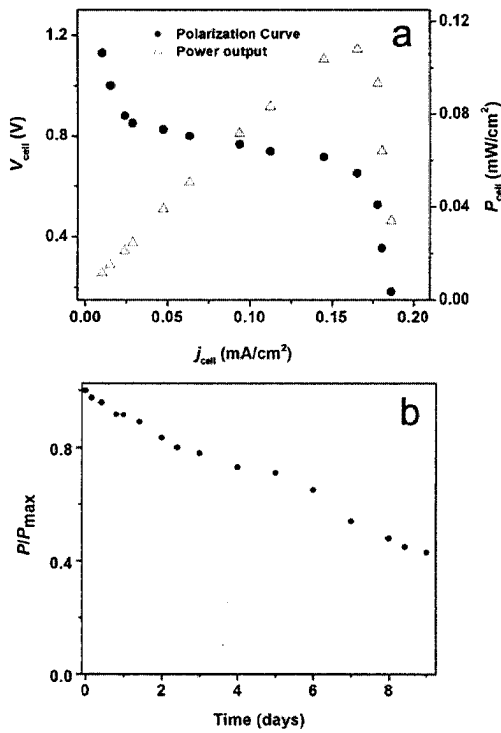


Figure 3. (a) Polarization curve of the assembled glucose/O₂ fuel cell and the dependence of the power output on the current density. (b) Stability of the assembled

biofuel cell. P is the power measured as a function of time, and P_{\max} is the maximum power value.

- 1 E. Katz, N. A. Shipway, I. Willner, W. Vielstich, A. Gasteiger, A. Lamm. *Fuel Cells - Fundamentals and Survey of Systems*, Wiley, London, 2003.
- 2 S. D. Minteer, B. Y. Liaw, M. J. Cooney, *Curr. Opin. Biotech.*, 2007, **18**, 228.
- 3 J. Kim, H. F. Jia, P. Wang, *Biotechnol. Adv.*, 2006, **24**, 296.
- 4 Y. M. Yan, W. Zheng, L. Su, L. Q. Mao, *Adv. Mater.*, 2006, **18**, 2639.
- 5 Y. Qiao, C. M. Li, S. J. Bao, Z. S. Lu, Y. H. Hong, *Chem. Commun.*, 2008, 1290.
- 6 S. Wu, H. X. Ju, Y. Liu, *Adv. Funct. Mater.*, 2007, **17**, 585.
- 7 M. E. G. Lyons, G. P. Keeley, *Chem. Commun.*, 2008, 2529.
- 8 A. Monnier, F. Schuth, Q. Huo, D. Kumar, D. Margolese, R. S. Maxwell, G. D. Stucky, M. Krishnamurty, P. Petroff, A. Firouzi, M. Janicke, B. F. Chmelka, *Science*, 1993, **261**, 1299.
- 9 J. Y. Ying, C. P. Mehnert, M. S. Wong, *Angew. Chem. Int. Edit.*, 1999, **38**, 56.
- 10 J. X. Jiang, F. Su, A. Trewin, C. D. Wood, H. Niu, J. T. A. Jones, Y. Z. Khimyak, A. I. Cooper, *J. Am. Chem. Soc.*, 2008, **130**, 7710.
- 11 S. Jun, S. H. Joo, R. Ryoo, M. Kruk, M. Jaroniec, Z. Liu, T. Ohsuna, O. Terasaki, *J. Am. Chem. Soc.*, 2000, **122**, 10712.
- 12 C. H. Kim, M. S. Khil, H. Y. Kim, H. U. Lee, K. Y. Jahng, *J. Biomed. Mater. Res. B*, 2006, **78**, 283.
- 13 X. J. Huang, H. S. Im, O. Yarimaga, J. H. Kim, D. Y. Jang, D. H. Lee, H. S. Kim, Y. K. Choi, *J. Electroanal. Chem.*, 2006, **594**, 27.
- 14 J. J. Feng, J. J. Xu, H. Y. Chen, *Biosens. Bioelectron.*, 2007, **22**, 1618.
- 15 S. J. Bao, C. M. Li, J. F. Zang, X. Q. Cui, Y. Qiao, J. Guo, *Adv. Funct. Mater.*, 2008, **18**, 591.